How to cite: *Angew. Chem. Int. Ed.* **2025**, *64*, e202421172
doi.org/10.1002/anie.202421172

Drug Discovery **Hot Paper**

Discovering Cell-Targeting Ligands and Cell-Surface Receptors by Selection of DNA-Encoded Chemical Libraries against Cancer Cells without Predefined Targets

Yuhan Gui, Rui Hou, Yuchen Huang, Yu Zhou, Shihao Liu, Ling Meng, Ying Li, Fong Sang Lam, Ruoyun Ding, Yan Cao, Gang Li, Xiaojie Lu,* and Xiaoyu Li**

Abstract: Small molecules that can bind to specific cells have broad application in cancer diagnosis and treatment. Screening large chemical libraries against live cells is an effective strategy for discovering cell-targeting ligands. The DNA-encoded chemical library (DEL or DECL) technology has emerged as a robust tool in drug discovery and has been successfully utilized in identifying ligands for biological targets. However, nearly all DEL selections have predefined targets, while target-agnostic DEL selections interrogating the entire cell surface remain underexplored. Herein, we systematically optimized a cell-based DEL selection method against cancer cells without predefined targets. A 104.96-million-member DEL was selected against MDA-MB-231 and MCF-7 breast cancer cells, representing high and low metastatic properties, respectively, which led to the identification of cell-specific small molecules. We further demonstrated cell-targeting applications of these ligands in cancer photodynamic therapy and targeted drug delivery. Finally, leveraging the DNA tag of DEL compounds, we identified α-enolase (ENO1) as the cell surface receptor of one of the ligands targeting the more aggressive MDA-MB-231 cells. Overall, this work offers an efficient approach for discovering cell-targeting small molecule ligands by using DELs and demonstrates that DELs can be a useful tool to identify specific surface receptors on cancer cells.

Introduction

In cancer treatment, it is crucial for therapeutic agents to effectively reach the tumor site and selectively bind to cancer cells. This binding specificity is essential to reduce systemic toxicity and enhance the efficacy of anti-cancer drugs. Therefore, the development of cell-specific ligands plays a significant role in cancer research.[1] Furthermore, the cell surface displays a variety of biomolecules arranged in complex structures that are unique to different cell types and properties, such as multimer assemblies, complexes, and microdomains.[2] Ligands capable of recognizing specific cell surface features can serve as valuable molecular probes for biomarker discovery and exploring the underlying signaling pathways.[1] While antibodies have traditionally been employed to target cell surface antigens,[3] they are large proteins that may encounter challenges such as stability issues, high manufacturing costs, incompatibility with oral administration, and potential organ toxicity and hypersensitivity reactions.[4]

Various combinatorial libraries, including phage display, mRNA display, yeast display, bacterial display, and one-bead one compound (OBOC) libraries, have been utilized to discover cell-targeting ligands through unbiased selections against live cells, tissue samples, ex vivo and in vivo systems, and even in humans.[5] However, the identified ligands primarily consist of peptides or peptidomimetics with less optimal pharmacokinetic properties.[5a] Cell-SELEX (systematic evolution of ligands by exponential enrichment) is a

[*] Y. Gui, R. Hou, Y. Zhou, S. Liu, L. Meng, Y. Li, F. Sang Lam, R. Ding, Prof. X. Li
Department of Chemistry and State Key Laboratory of Synthetic Chemistry, The University of Hong Kong, Pokfulam Road, Hong Kong SAR, China
E-mail: xiaoyuli@hku.hk

Y. Gui, R. Hou, Y. Zhou, L. Meng, F. Sang Lam, Prof. X. Li
Laboratory for Synthetic Chemistry and Chemical Biology Limited, Health@InnoHK Innovation and Technology Commission, Units 1503-1511, 15/F., Building 17 W, Hong Kong SAR, China
E-mail: xiaoyuli@hku.hk

Prof. X. Lu
State Key Laboratory of Drug Research, Shanghai Institute of Materia Medica, Chinese Academy of Sciences, 501 Haike Road, Zhang Jiang Hi-Tech Park, Pudong, Shanghai 201203, P. R. China
E-mail: xjlu@simm.ac.cn

Y. Huang, Prof. G. Li
Institute of Systems and Physical Biology, Shenzhen Bay Laboratory, Shenzhen, China
E-mail: ligang@szbl.ac.cn

Prof. Y. Cao
School of Pharmacy, Naval Medical University, Shanghai 200433, China

Y. Zhou
Present address: Institute of Translational Medicine & School of Basic Medicine and Clinical Pharmacy, China Pharmaceutical University, Nanjing, China, 211198

powerful technique for identifying cell-binding aptamers,[6] yet it is limited to nucleic acid structures. While small molecules exhibit more favorable drug-like properties and are more synthetically manageable, effective methods for identifying cell-targeting small molecules, particularly in a high-throughput manner, remain scarce. Furthermore, despite the discovery of numerous cell-targeting peptides and aptamers through unbiased selections against cancer cells, with some already approved for clinical use, it is striking that only a small fraction of these ligands has had their cellular receptors identified.[2,5a,6b,7] Target identification falls far behind ligand discovery, representing a significant challenge in the biological and clinical advancement of these ligands.

Originally proposed by Brenner and Lerner in 1992[8] and experimentally demonstrated by Janda in 1993,[9] DNA-encoded chemical library (DEL or DECL) has since become a powerful platform widely used in drug discovery.[10] In a DEL, each compound is encoded with a unique DNA tag, which allows the synthesis, processing, and selection of millions to billions of compounds simultaneously at minute scale. The selected binders are decoded by PCR amplification and next-generation sequencing (NGS) (Figure 1a). With the rapid development of DNA-compatible reactions, the chemical space of DELs has been greatly expanded.[10g,l,r,v,11] DELs have been used to interrogate numerous protein and nucleic acid targets. DEL selections on and inside live cells have also been realized.[12] The Bradley group pioneered PNA-encoded library screening on live cells;[13] GSK reported the first cell-based DEL selection with cells overexpressing tachykinin receptor neurokinin-3;[12a] the Krusemark group applied a crosslinking method[14] to both cell-surface and intracellular targets;[12b–d] the Neri group extensively optimized the experimental conditions for cell-surface selections;[12e] Vipergen microinjected both the library and the target's mRNA into frog oocytes to enable intracellular selection;[12f] our group developed DEL selection methods against endogenous membrane proteins;[12g–i] and Kodadek, Paegel, and co-workers selected an OBOC-DEL library against antibodies in human sera from patients with active or latent tuberculosis (TB) to identify ligands specific for active TB IgG antibodies.[15] However, nearly all DEL selections have predefined targets, whereas completely unbiased, target-agnostic selections remain largely unexplored. Very recently, GSK reported DEL selections against mouse myoblast and myotube cells, as well as human lymphocytes;[16] however, the receptors of the identified cell-selective ligands were not identified and the compounds were not used in cell-targeting applications.

In principle, DEL selections should be an efficient approach for identifying cell-targeting ligands. First, DELs contain high chemical diversity that can be sampled by the complex landscape of the cell surface.[17] Second, the DNA conjugation site of DEL compounds provides a convenient exit vector to attach payloads and labels for biological applications. Third, DEL selections avoid the avidity effect from multivalent binding, which is often seen with phage display and OBOC libraries.[18] Herein, we report a method for conducting unbiased DEL selections on live cells without predefined targets. This approach involves utilizing photo-crosslinking to stabilize the interactions between ligands and receptors on the cell surface. (Figure 1b).[12b–d,g,14,19] After systematically optimizing the selection conditions, we selected a 104.96-million-member DEL against MDA-MB-231 and MCF-7, a pair of breast cancer cells presenting different metastatic properties.[2,5a,7,20] Small molecule ligands specifically targeting the more aggressive MDA-MB-231 cells with double-to- single-digit micromolar affinities have been identified, which were used to guide the selective killing of MDA-MB-231 cells via photodynamic therapy and targeted

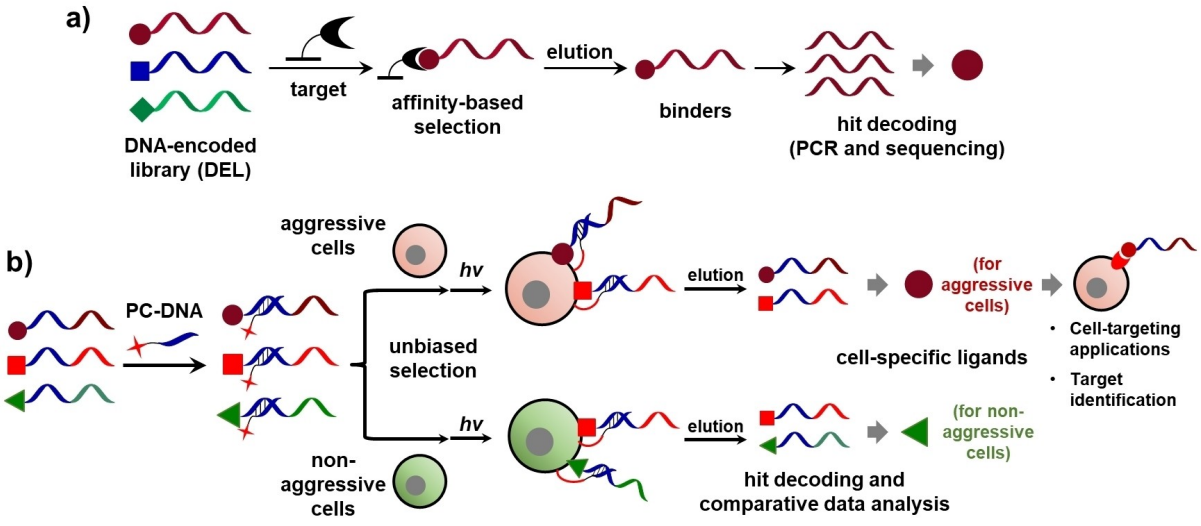

Figure 1. DEL selection against immobilized targets and the proposed unbiased selection on live cells. a) DEL selection with immobilized targets. b) This work: Unbiased DEL selection on live cells without predefined targets. Photo-crosslinking is used to stabilize ligand-receptor binding. Selection results from different cells are compared to identify cell-specific ligands, which can be used for cell-targeting applications and target ID to identify the corresponding receptors. PC-DNA: photo-crosslinking DNA; red star: photo-crosslinker.

drug delivery. Furthermore, by leveraging the DNA tag of DEL compounds, we performed target identification (target ID) of compound **5**, one of the MDA-MB-231 specific ligands, and identified α-enolase (ENO1) as the cell surface receptor of compound **5**. We further validated that compound **5** is an α-enolase inhibitor, thereby reducing the migration of MDA-MB-231 cells. Collectively, this study has demonstrated that DEL selection is an efficient method for discovering cell-targeting small molecules as well as cell surface receptors as potential biomarkers.

Results and Discussion

Development of the Unbiased DEL Selection Method on Live Cells

In DEL selections, the target-ligand binding equilibrium is driven by the high target concentration. For selections against the cell surface without a predefined target, the techniques to increase the effective target concentration, such as protein overexpression and tagging,[12] can no longer be used. If the cells are simply incubated with the library and subjected to the washing steps, then only the strong binders to the targets of high abundance will be identified, while the moderate binders and possibly even high-affinity ligands binding to low-abundance targets would be lost. Therefore, we hybridized a photo-crosslinking DNA (PC-DNA) at the primer-binding site of the library (Figure 1b). Upon UV irradiation, the PC-DNA covalently captures the target, thereby stabilizing ligand-receptor interactions. After washing, the binders can be eluted from the cell under denaturing condition for hit decoding. Such a crosslinking technique has been proven to improve the library recovery and facilitate the identification of moderate and low-affinity binders in DEL selections.[12b–d,h,i,14,19,23] The library will be selected in parallel against cells with different properties (e.g., aggressive vs. non-aggressive; Figure 1b). The enrichment profiles will be compared to identify the cell-specific ligands, which can be further utilized for cell-targeting applications and identifying the cell surface receptors.

While this study aims to achieve "targetless" selections against the entire cell surface, we reasoned that starting with a known target would facilitate methodology development. As shown in Figure 2a, CA-12 (carbonic anhydrase 12) is a membrane carbonic anhydrase implicated in malignant cancers,[24] and **CBS** (*p*-carboxybenzene sulfonamide) is a known ligand of CA-12 ($K_d = 0.97$ μM in DNA-conjugated form).[12h,23a,25] A549 cells expressing CA-12 were used as the target cells, and the effective concentration of CA-12 was determined to be ~1.04 μM (Figure S1). First, **CBS** was covalently tethered to a 16-nt DNA as the binding probe (BP) (**BP-1**). A complementary 16-nt DNA carrying the photo-reactive phenylazide group and a biotin tag was prepared as the capture probe (CP) (**bio-CP-1**; Figure 2a). The **BP-1/bio-CP-1** duplexes were incubated with A549 cells (4 °C, 90 min.) and then briefly UV-irradiated (365 nm, 1 min.). After washing, the binders were eluted by heating, isolated with avidin beads, and analyzed by western blot,[23a] showing specific labeling of CA-12 (Figure 2b and S2). By replacing the biotin with a fluorescein group (FAM) (**fam-CP-1**), flow cytometry analysis corroborated the specific labeling (Figure 2c). Next, we optimized the selection conditions to maximize the enrichment fold (EF). **CBS** was conjugated to a 35-nt DNA (**BP-2**), and an amine-modified DNA with orthogonal primer-binding sites was used as the background (**NP-2**). The DNAs were mixed (1:10) and hybridized with a 16-nt CP (**CP-2**). The model library was selected against A549 cells (Figure 2d), and quantitative PCR (qPCR; Figure S3) was used to quantify **CBS** enrichment. First, an incubation time of at least 1.5 h and a 2-step washing procedure are beneficial in improving library recovery and enrichment fold (Figure 2e-2f). The number of cells used in the selection had little effect, consistent with the previous report (Figure 2g).[26] Blocking agents (NaN_3 and sheared salmon sperm DNA) are often used to minimize non-specific interactions in DEL selections.[27] Interestingly, here they decreased the EF values (Figure 2h). Running multiple rounds of selections, i.e., the eluted binders are directly used as the input for the next round, is frequently employed to improve enrichment; we also observed that two rounds of selections gave significantly better results (Figure 2i). Next, we increased the **BP-2**/**NP-2** ratio to 1:7,000 and performed the selection under the optimized conditions. A ~200 EF was obtained after 2 rounds of selections (Figure 2j and S4). Unfortunately, an additional round of selection led to insufficient amount of recovered library, giving C_T's falling outside the reliable range (Figure S4). Furthermore, a model library with chemical diversity was prepared by mixing a **CBS**-DNA conjugate with a 67,600-member dipeptide DEL (equal ratio for each compound; Figure 2k).[28] The 67,601-member library was selected against A549 cells, and the selected compounds were PCR-amplified with the NGS-compatible primers and analyzed with NGS (Figure S5). The raw sequencing data were processed by using a Python script to quantitatively tally the codons of each compound and then calculate the enrichment fold (post-selection% /pre-selection%), which generated a 2D scatter plot for each selection (enrichment fold vs. post-selection sequencing count).[21] The data points with both high enrichment folds and sequencing counts are considered to be potential hits. **CBS** gave low EF after the 1st round of selection but was significantly enriched after the 2nd round (Figure 2l). Low enrichment was also observed without photo-crosslinking. Next, we performed a counter-selection against HEK293 cells, a cell line with low CA-12 expression. The *z*-scores of the enriched compounds[22,29] of the two cell lines were plotted, and it showed the preferential enrichment of **CBS** on A549 cells (Figure 2m). Moreover, we also tested the selection with another model system. Folate receptor (FR) is a cell-surface glycoproteins implicated in cancers. Folate acid (**FA**) is a nanomolar binder of FR.[23a] A model library was prepared by mixing a **FA**-DNA conjugate with excess background DNA and selected against HeLa cells over-expressing FR.[23a] qPCR analysis showed significant enrichment of the **FA**-DNA conjugate (Figure S6).

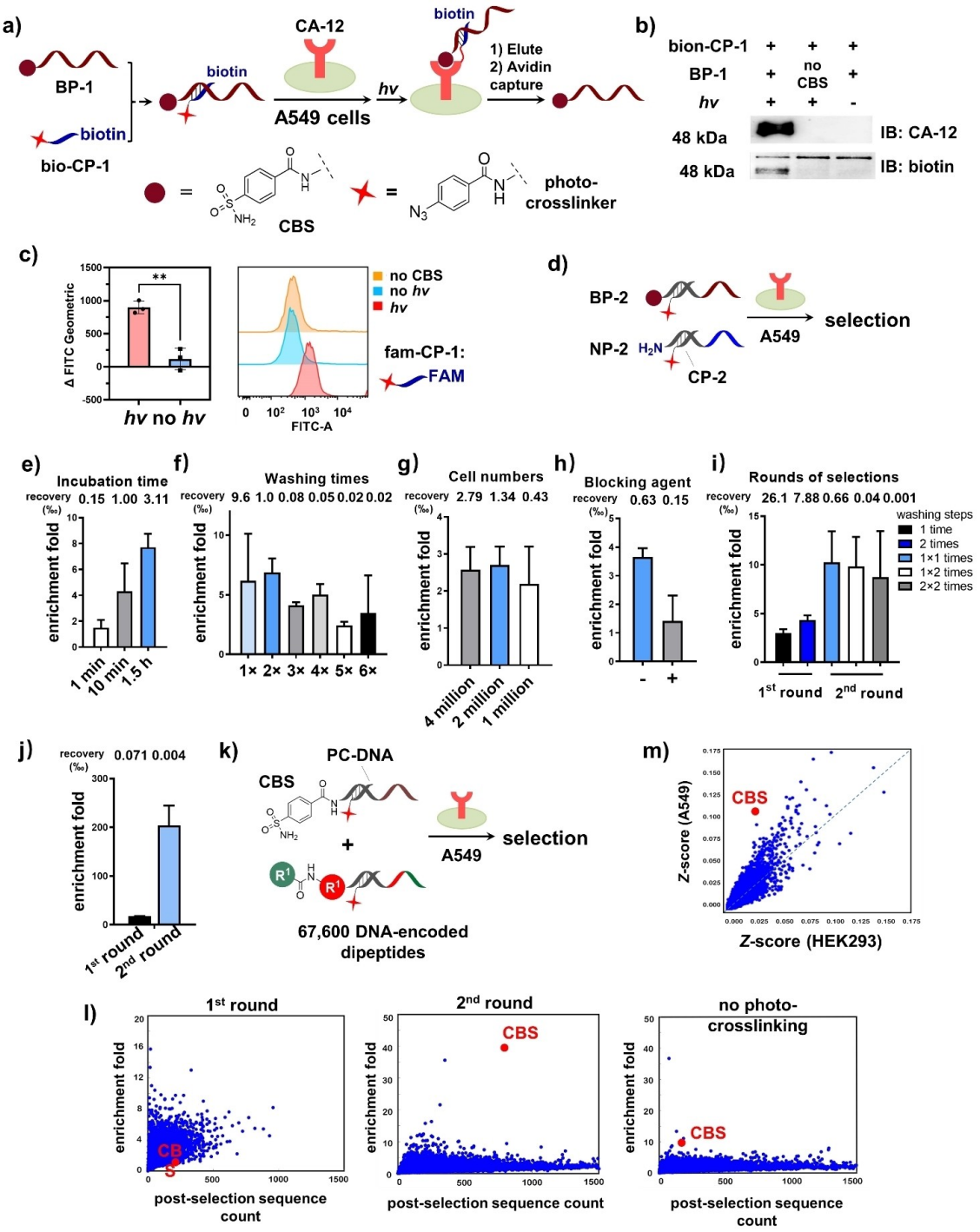

Figure 2. Selection method optimization. a-c) **BP-1** was hybridized with **bio-CP-1** or **fam-CP-1**. The duplexes were used to label CA-12 on A549 cells. After photo-crosslinking, washing, and elution, the labeled proteins or cells were analyzed by using b) western blot and c) flow cytometry. In (b), no **CBS**: no **CBS** in **BP-1**. Conditions: DNA, 5 μM; number of cells, 2 million; buffer, 1x phosphate-buffer saline (PBS); UV, 365 nm, 60 s. at 0 °C; IB, immunoblotting. d) A model library was selected against A549 cells under different conditions: e) incubation time; f) number of washes; g) number of cells; h) use of blocking agents (0.1 % NaN_3 (g/100 mL) and 1 % sheared salmon sperm DNA); and i) rounds of selections. The selections were analyzed with qPCR to calculate the library recovery and the enrichment fold (EF) of **BP-2**. j) Selection result of a 1 : 7,000 model library. k) A model library containing 67,000 dipeptides and **CBS-DNA** was selected against A549 cells. l) NGS sequencing results shown in scatter plots.[21] *y*-axis: enrichment fold; *x*-axis: post-selection sequencing counts; enrichment fold: post-selection% /pre-selection% (naïve library). **CBS-DNA** are highlighted. m) Comparison of the normalized *z*-score of the enriched compounds in A549 (*x*-axis) and HEK293 selections (*y*-axis).[22] The statistical data are presented as the mean values ± s.d. and analyzed using the two-tailed unpaired t-test. (** $p < 0.01$; $n = 3$ in c) and $n = 2$ in d)-j) independent experiments)

Unbiased Selections Against MDA-MB-231 and MCF-7 cells and Hit Validation

Two breast cancer cell lines were chosen for the selection: MDA-MB-231 and MCF-7. MDA-MB-231 is a highly aggressive and poorly differentiated cell line established from metastatic pleural effusion of mammary adenocarcinoma;[30] MCF-7 cells were also derived from pleural effusion but are significantly less aggressive.[31] The pair of cells has been used as "positive" and "negative" cells in many profiling and library screening studies.[2,5a,7,20] First, we validated the different metastatic phenotypes of the cell lines (Figure S7). Next, a 104.96-million-compound DEL consisting of three sets of building blocks (BBs) was prepared. The library was synthesized by first coupling 321 amino acids (R^1) to the amine-modified "headpiece" DNA, followed by 326 amino acids (R^2) to form the dipeptides. Finally, 640 carboxylic acids were coupled via amidation, 330 aldehydes were coupled via reductive amination, 33 sulfonyl chlorides and heterocyclic chlorides were coupled via nucleophilic addition and nucleophilic substitution reactions, respectively. (total 1,003 R^3 BBs) (Figure 3a and S8). The library, originally encoded with double-stranded DNA (dsDNA), was converted to single-stranded DNA (ssDNA) by *Lambda* exonuclease digestion (Figure 3b).[12h] After hybridizing a 15-nt PC-DNA at the primer-binding site, the library was selected against MDA-MB-231 and MCF-7 cells, respectively, and the eluted binders were PCR-amplified and decoded with NGS. The selection experiments were performed in triplicates. The raw sequencing data were first processed using a previously reported method[32] to count the number of the sequence reads for each library compound. Using a custom script (section 8 in the Supporting Information), the z-score of each compound was obtained based on an optimized binomial distribution model.[33]

We focused on the compounds more significantly enriched by the aggressive MDA-MB-231 cells. The z-scores of the compounds with a post-sequencing count >200 in MDA-MB-231 selections were plotted (MDA-MB-231 vs. MCF7; three replicates shown in Figure 3c). Next, hit compounds were chosen if they are reproducible in at least two out of the three replicates.[12i] A total of 109 compounds fit this criteria (full list in Figure S9). The top 7 compounds with the highest average z-scores were selected for hit resynthesis and validation (Figure 3c-3e).

Next, the selected hit compounds were resynthesized on a 16-nt ssDNA (**DNA-1** to **7**) and hybridized with **fam-CP-1**. The duplexes were used to label MDA-MB-231 and MCF-7 cells, respectively, and the labeling efficiencies were analyzed with flow cytometry. As shown in Figure 4a and S10, all compounds gave significantly higher fluorescence signal on MDA-MB-231 cells than on MCF-7 cells. Moreover, titration experiment showed that the compounds labeled the cells in dose-dependent manner, and their binding affinities (K_d) to MDA-MB-231 cells were estimated to be in the single- to double-digit micromolar range (Figure 4b and S11). Compounds **5** and **6** exhibited relatively higher affinities. We first chose compound **5** for further studies due to the potential instability of the iodobenzene motif of **6** under UV.[34] As shown in Figure 4c-4d, **DNA-5** exhibited little binding to MCF-7 cells, similar to **DNA-OH**, a DNA strand without the conjugated small molecule. The binding specificity of **DNA-5** was also observed with confocal microscopy (Figure 4e). Interestingly, when MDA-MB-231 cells were pre-treated with proteinases (proteinase K or trypsin),[35] **DNA-5**'s binding was almost completely abolished (Figure 4f), suggesting that the cell-surface receptors of **DNA-5** are likely to be proteins. Collectively, these results have proved that the identified hit compounds specifically bind to MDA-MB-231 cells.

Identification of the Cell Surface Receptor of Compound 5

Next, we performed target ID of compound **5** on MDA-MB-231 cells by leverage the DNA tag. Previously, we reported a DNA-programmed affinity labeling (DPAL) method,[36] which has been utilized to identify the targets of various small molecules and nucleic acids.[37] The DNA conjugate of compound **5** was hybridized with three complementary biotinylated CPs, in which the photo- cross-linker is either protruding by three nucleobases ($n=+3$), side-by-side ($n=0$), or recessive ($n=-3$) relative to the small molecule (Figure 5a and S12). Previously, we have shown such a multi-probe approach is beneficial for target identification, as it can present different probe configurations to increase the likelihood of identifying the binding targets.[36,38] The affinity probes were incubated with MDA-MB-231 cells and UV-irradiated, before the cells were lysed by heating. The captured proteins were isolated with streptavidin beads and analyzed by western blot. The results showed two protein bands with molecular masses of ~50–60 kDa were specifically captured, which disappeared with free compound **5** competition (100 μM) (Figure 5b). Furthermore, we performed quantitative proteomic analysis of the captured proteins by using Stable Isotope Labeling with Amino acids in Cell culture (SILAC).[39] In brief, the cells were cultured with "heavy" and "light" isotopes, respectively; then, the heavy/light cells were incubated with the probes either with or without free small molecule competition. The experiments were performed reciprocally with five replicates. The captured protein samples were trypsin-digested and submitted for proteomic analysis. The heavy/light ratios for each of the identified proteins were calculated and plotted (Figure 5c and full data in Figure S13–S17). One protein, α-enolase (ENO1), has been clearly enriched in all five replicates, while another protein glyceraldehyde-3-phosphate dehydrogenase (GAPDH) has been identified in four replicates. The molecular weight of α-enolase is ~48 kDa, matching the protein bands in the pulldown experiments in Figure 5b. Therefore, we repeated the pulldown experiments in Figure 5a, and the captured proteins were isolated and probed with an anti-α-enolase antibody. The result showed that α-enolase was specifically captured by compound **5** and the capture can be abolished with free compound **5** competition or without photo-cross-linking (Figure 5d–5e). Next, we established an MDA-MB-

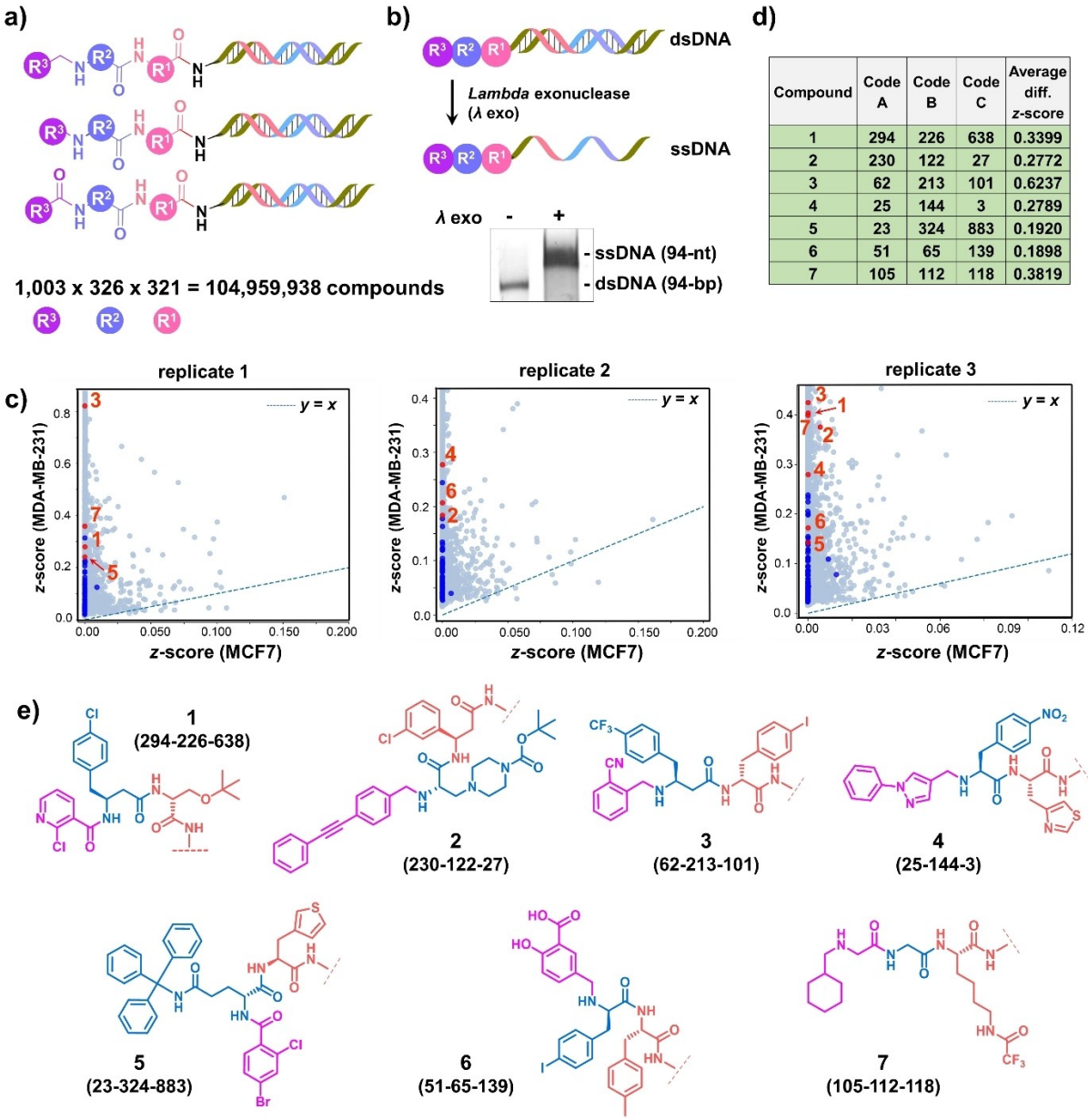

Compound	Code A	Code B	Code C	Average diff. z-score
1	294	226	638	0.3399
2	230	122	27	0.2772
3	62	213	101	0.6237
4	25	144	3	0.2789
5	23	324	883	0.1920
6	51	65	139	0.1898
7	105	112	118	0.3819

Figure 3. Selection of an approximately 104.96-million DEL against MDA-MB-231 and MCF-7 cells. a) Structure and BB composition of the library. b) Converting the dsDNA tag to ssDNA by using *Lambda* exonuclease.[12h] Gel image shows the band shift after the conversion (6% denaturing PAGE). c) Scatter plots showing the *z*-scores of the compounds with a post-selection sequence count > 200 in MDA-MB-231 selections; three independent replicates are shown. *y*-axis: MDA-MB-231; *x*-axis: MCF-7; dashed line: $y = x$. The compounds enriched in at least two of the three replicates are highlighted in blue; the top 7 compounds with the highest average *z*-scores in MDA-MB-231 selections are highlighted in red. See the Supporting Information for details on data analysis, *z*-score calculation, and hit selection. Sequencing data and the *z*-score calculation source data are provided in the Supporting Information and deposited in figshare (DOI: 10.25442/hku.28022942). d) Table showing the average *z*-scores of the top 7 compounds. See Figure S9 for the full list. Average diff. *z*-score: the average of the diff. *z*-score values from the biological replicates. diff. *z*-score: *z*-score difference between the MDA-MB-231 and MCF-7 selections in each replicate. e) Structures of the top 7 hit compounds. BB numbers are shown in brackets. See the Supporting Information for details on library synthesis, selection, and data analysis (Figures S8 and S9).

231 cell line stably expressing shRNAs targeting the ENO1 gene (shENO1; Figure 5f) and examined the binding of compound **5** to the ENO-1 knocked down cells by flow cytometry. As shown in Figure 5g, shENO1-expressing cells exhibited significantly reduced binding to compound **5**, as compared with the cells expressing a control shRNA with scrambled sequences. Furthermore, to verify the direct interaction between compound **5** and α-enolase, we employed three different biophysical methods, surface plasmon resonance (SPR), microscale thermophoresis (MST), and fluorescence polarization (FP), and confirmed that compound **5** binds to α-enolase (Sino Biological, recombinant human ENO1 protein (His-Tag), cat.#: 11554-H07E) at nanomolar affinity (123 to 161 nM; Figure 5h). In the FP

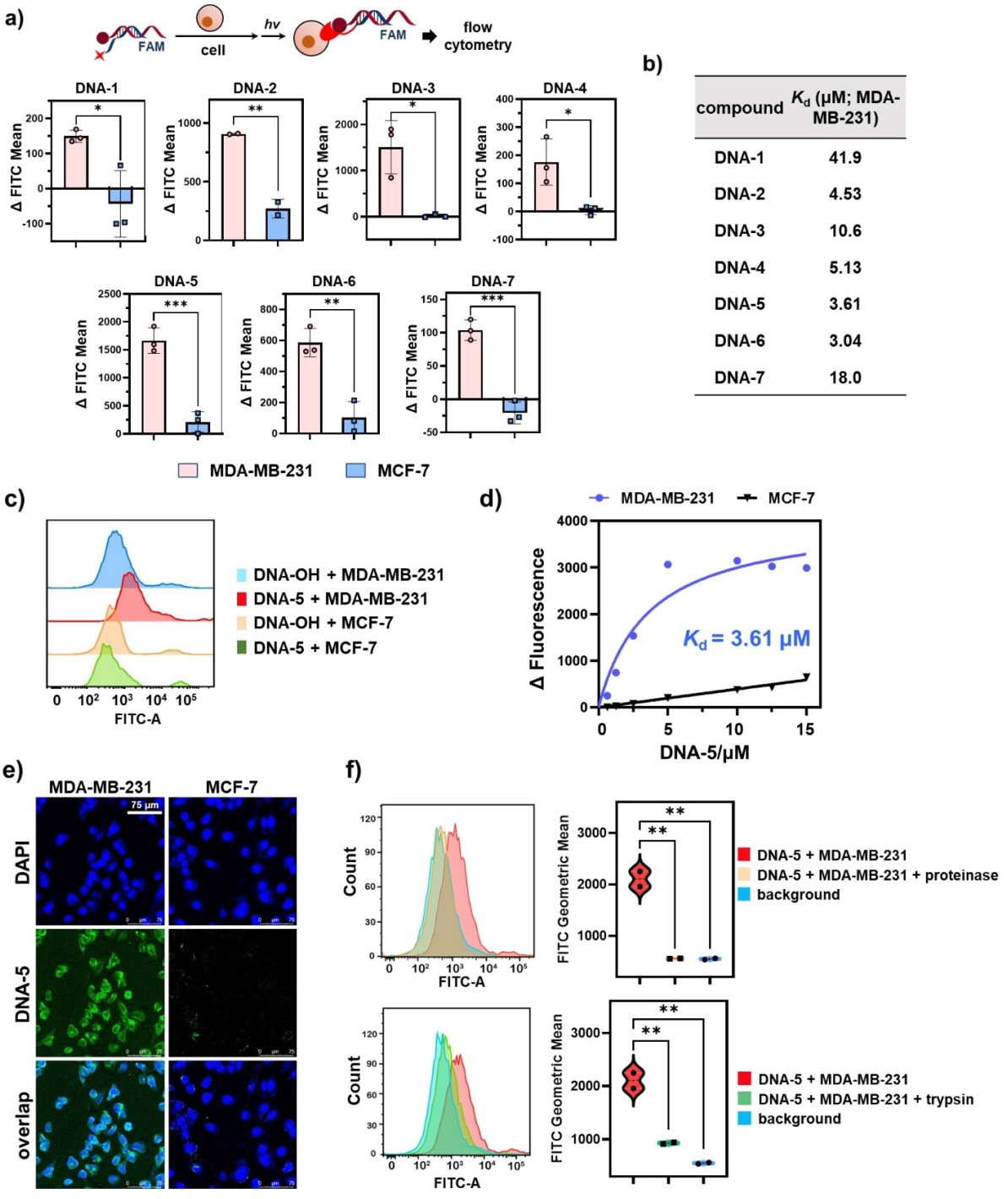

compound	K_d (μM; MDA-MB-231)
DNA-1	41.9
DNA-2	4.53
DNA-3	10.6
DNA-4	5.13
DNA-5	3.61
DNA-6	3.04
DNA-7	18.0

Figure 4. The on-DNA hit compounds bind specifically to MDA-MB-231. a) **DNA-1** to **7** were hybridized with **fam-CP-1** and the duplexes were used to label MDA-MB-231 and MCF-7 cells, respectively. The labeling efficiencies were analyzed with flow cytometry; histograms are provided in Figure S10. ΔFITC mean was obtained from the mean fluorescence intensity of the DNA conjugates subtracted with the mean fluorescence background from the control without small molecule (DNA-OH). b) The binding affinities of **DNA-1** to **7** to MDA-MB-231 cells, determined by flow cytometry. Fitting curves are provided in Figure S11. c) Flow cytometry analysis of the labeling efficiencies of **DNA-5** and **DNA-OH** on MDA-MB-231 and MCF-7 cells. d) Comparison of the binding affinities of **DNA-5** and **DNA-OH** to MDA-MB-231 cells. e) Confocal imaging analysis of **DNA-5**'s labeling of MDA-MB-231 and MCF-7 cells. DAPI: 4′,6-diamidino-2-phenylindole. f) Flow cytometry analysis of **DNA-5**'s binding to proteinase K- and trypsin-treated MDA-MB-231 cells. Right panels: violin plots showing the FITC signal of the labeling reactions. The statistical data are presented as the mean values ± s.d. and analyzed using the two-tailed unpaired t-test (for a) and one-way ANOVA with Tukey's tests (for f) (* $p < 0.05$; ** $p < 0.01$; *** $p < 0.001$; $n = 3$ in a) except **DNA-2** ($n = 2$) and $n = 2$ in f) independent experiments).

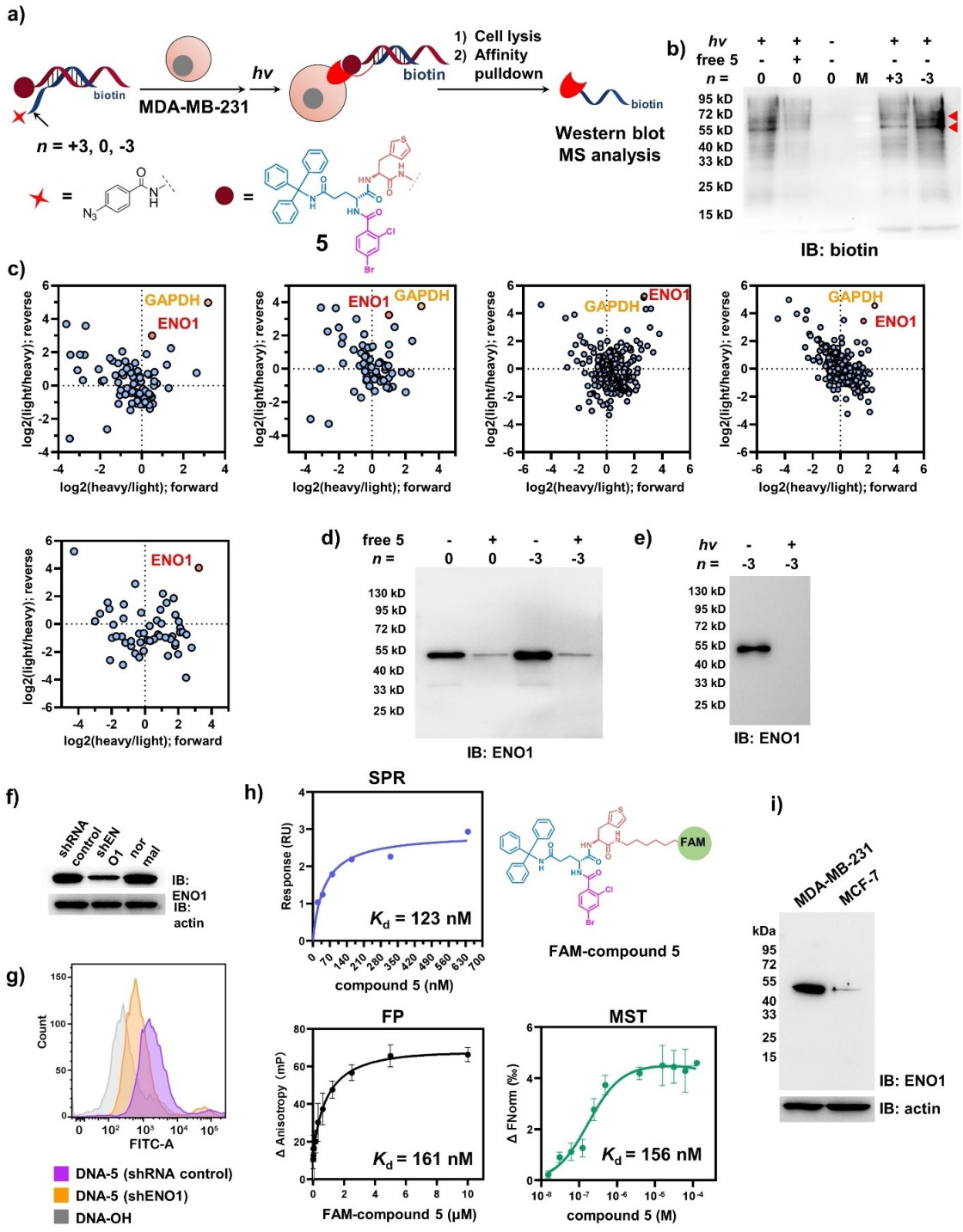

Figure 5. Target ID **of** compound **5**. a) DPAL-mediated identification of cell-surface receptors of compound **5**.[36,38] b) western blot analysis of the captured proteins. M: marker; free 5: with free compound **5** (100 μM); *n*: number of nucleobases in the spacer; red triangles mark the potential target bands. c) SILAC-based proteomic MS analysis of the captured proteins. Five biological replicates were performed. *x*-axis: $\log_2$(heavy/light ratio) of the "*forward*" experiments; *y*-axis: $\log_2$(light/heavy ratio) of the "*reverse*" experiments. The proteins enriched in the upper right quadrant are potential hits. d,e) western blot analysis of the captured proteins using anti-ENO1 antibody (with and without free compound **5**; with and without UV). F) Measurement of the "off-DNA" binding affinity of compound **5** to ENO1 using SPR, MST, and FP. In FP, a FAM-labeled compound **5** was used. Except in SPR, g) knocking down ENO1 by using short hairpin RNAs targeting ENO1 (shENO1); shRNA control: scrambled sequences. h) Flow cytometry analysis of the **DNA-5** labeling efficiency of MDA-MB-231 cells, either expressing shENO1 or the shRNA control. **DNA-OH**: a negative control DNA without conjugated small molecule. The labeling experiments are the same as described in Figure 4. i) Membrane-associated ENO1 of MDA-MB-231 and MCF-7 cells were isolated and analyzed by western blot. See the Supporting Information for details. The statistical data in (h) are presented as the mean values ± s.d. ($n = 3$ independent experiments).

experiments, a FAM-compound 5 conjugate was used. The K_d values of compound **5** from the biophysical assays are smaller than the one from flow cytometry (Figure 4b), which may be due to several factors. First, biophysical assays measure the binding between the small molecule and the purified ENO1. In flow cytometry, the target is the entire cell surface; therefore, the K_d value is an "average" of a multitude of different interactions with a wide range of affinities, exhibiting apparent weaker binding for the DNA-conjugated small molecules. Second, DNA conjugation may interfere with small molecule's binding due to steric hindrance and/or the limited binding poses from the relatively large DNA molecule.[23a] Third, the ENO1 protein on the cell surface may be in different conformations than the purified protein and/or form complexes with other membrane proteins. Biophysical assay results better reflected compound **5**'s affinity to ENO1, while the cell-based flow cytometry experiments can be used as a rapid method for preliminary "on-DNA" hit validation.[40] Finally, we also verified that MDA-MB-231 cells have higher level of cell-membrane-associated α-enolase than that of MCF-7 cells (Figure 5i).[41] Taken together, these results have shown that α-enolase is a direct binding target of compound **5** on MDA-MB-231 cells.

α-enolase is commonly known as a glycolytic enzyme in the cytosol catalyzing the conversion of 2-phosphoglycerate to phosphoenolpyruvate (PEP), but it also "moonlights" on the cell surface, acting as a plasminogen receptor and activator and promoting cell migration.[42] α-enolase contributes to cancer cell proliferation, migration, invasion, and metastasis and is a promising anti-cancer drug target.[42,42,43] To investigate whether compound **5**'s binding affects α-enolase's biological activities, we first verified that no significant cytotoxicity was observed for compound **5** at the concentration up to 100 μM (Figure S18). Next, transwell assays showed that compound **5** significantly inhibited MDA-MB-231 cell migration at 20 μM, similar to **AP-III-a4** at 10 μM, which is a known enolase inhibitor with a reported IC_{50} of 576 nM (Figure 6a–6b).[44] Moreover, we tested compound **5**'s inhibitory activity by using an enolase activity assay, in which the substrate 2-phosphoglycerate is converted to PEP by the enzyme, resulting an intermediate product that reacts with a peroxidase substrate to generate a fluorometric product. As show in Figure 6c, an IC_{50} value of 21.6 μM was obtained for compound **5**, and **AP-III-4** also gave a modest IC_{50} of 20.4 μM, suggesting high substrate concentration in the assay. By using the Cheng–Prusoff equation[45] and based on the reported kinetic parameters of α-enolase.[46] the inhibition constant (K_i) of compound **5** is calculated to be ~0.569 μM, comparable to its binding affinity.

The trityl group is highly lipophilic and may bind to the hydrophobic patches on different proteins non-selectively. In compound **5**, the trityl-bearing motif is part of the R2 building block in the library. Since the library was synthesized by using the split-mix procedure (Figure 3a), there are many other compounds containing the same R^2 but different R^1/R^3 combinations. However, they were not identified or significantly enriched in the selection with MDA-MB-231 cells. Thus, we postulate that the combination of the trityl group with the other building blocks brings some degree of binding selectivity. We synthesized two derivatives of compound **5** (Figure S19), in which either the trityl group is removed or the R^1 and R^3 flanking the trityl group are changed to different structures. As shown in Figure S19, no ENO1 binding was observed with the two derivatives. Furthermore, we measured the binding of compound **5** to several unrelated proteins and also a peptide including COX2 (cyclooxygenase-2), CA-2 (carbonic anhydrase 2), SIRT1 (Sirtuin 1), and His-tag. Again, no binding was observed (Figure S19). These results suggested that compound **5** has a certain degree of selectivity in binding to ENO1. Nevertheless, it is important to note that the trityl group is likely to incur non-specific interactions when encountering a wider range of proteins on different cell types.

The SILAC results showed that GAPDH was captured by compound **5** in four replicates (Figure 5c). GAPDH is an important enzyme in the glycolytic pathway. Interestingly, it is also a "moonlighting" protein that can be trafficked to cell membrane performing other biological functions, such as transferrin receptor on mammalian cells[47] and binding to human vitronectin and plasminogen on bacterial cells.[48] However, no binding of compound **5** to the purified GAPDH was detected in both SPR and MST experiments (Figure S20).

Moreover, knocking down GAPDH did not have noticeable effect on the binding of compound **5** to the cell surface (Figure S21). Compound **5** also showed no inhibitory activity in GAPDH biochemical assays (Figure S22). These results suggested that GAPDH may not be a direct target of compound **5** on MDA-MB-231 cells, at least not with an appreciable binding affinity. However, it is puzzling that it was enriched in SILAC experiments. Thus, we used a cell surface protein isolation kit and compared the cell-membrane-associated GAPDH levels and observed significantly higher levels on MDA-MB-231 cells (Figure S23). Furthermore, the effective concentration of GAPDH on MDA-MB-231 cells is very high (~43.7 μM); for comparison, the cell surface α-enolase is ~5.93 μM (Figure S24). Taken together, we hypothesize that the enrichment of GAPDH might be due to its high concentration on MDA-MB-231 cells, despite the weak binding affinity. Alternatively, GAPDH has been reported to directly interact with ENO1;[49] therefore, it may get labeled by the compound **5** probe in a proximity manner as we observed previously.[38] In addition, it is also possible that the cell-surface GAPDH may present some special conformation or complex assembly that can bind to compound **5** more strongly than in the purified form; however, it is unlikely since the shRNA knock-down experiments (Figure S21) indicated that GAPDH-ligand interaction did not significantly contribute the overall ligand binding. Nevertheless, these results highlight the importance of validation of the target after identification.

Furthermore, we performed the same target identification experiments with compounds **2**, **3**, **4**, and **6** (Figure S25a), which showed relatively high binding affinities among the selected compounds. The SILAC experiments

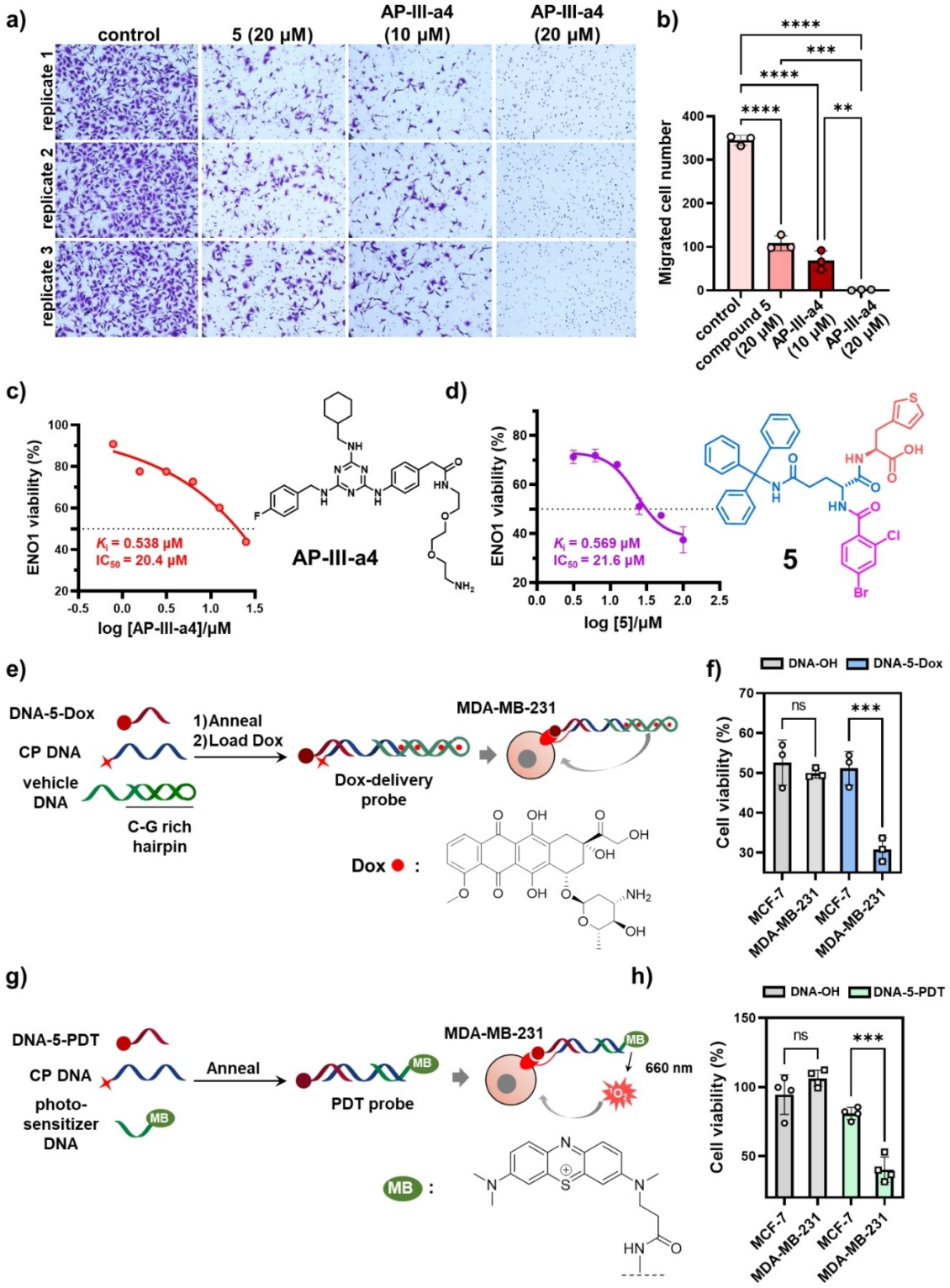

Figure 6. Biological activities and applications of compound **5**. a) Compound **5** inhibited MDA-MB-231 cell migration in transwell assays; three replicates are shown. b) Column graph summarizing the results in a). c,d) Titration curve of the positive control **AP-III-a4** and compound **5** in the α-enolase enzymatic activity assay. e) Delivery of Dox using the probe assembled from DNA-conjugated compound **5** (**DNA-5-Dox**), a photo-reactive CP DNA, and a C–G rich vehicle DNA. f) Cell viability after Dox delivery using the probe shown in (d). g) PDT treatment of cells using probes assembled from DNA-conjugated compound **5** (**DNA-5-PDT**), a photo-reactive CP DNA, and a PS-DNA. g) Cell viability after PDT treatment with the probe shown in (h). **DNA-OH**: control probe without conjugated compound **5**. In (e) and (g). The statistical data are presented as the mean values ± s.d. and analyzed using the one-way ANOVA with Tukey's tests (** $p < 0.01$; *** $p < 0.001$; **** $p < 0.0001$; $n = 3$ in (b), $n = 2$ in (d), $n = 3$ in (f), and $n = 4$ in (h) independent experiments).

were performed in duplicates and the results showed that the DNA-small molecule conjugates (**DNA-2**, **3**, **4**, and **6**) did not capture ENO1 or GAPDH (Figure S25b-e and S26–S33), indicating that these compounds do not bind to α-enolase or GAPDH. Moreover, compounds **2**, **3**, and **4** captured different proteins (**2**: FAR1; **3**: DARS2, COQ8 A, AIFM2; **4**: FHL1), suggesting that they may have different targets on MDA-MB-231 cells, which will be further characterized in future studies. Interestingly, **DNA-6** did not reproducibly capture any proteins (Figure S25f). Thus, we paired **DNA-6** with a FAM-labeled CP and compared the binding of **DNA-6** to MDA-MB-231 cells with and without trypsin digestion by using flow cytometry. The results showed that trypsin digestion did not significantly reduce the fluorescence signal, suggesting that compound **6** may bind to non-protein molecules on the cells surface (Figure S25g).[50]

Cell-targeting Applications of Compound 5

Cell-specific ligands can be used in a variety of applications targeting cancer cells, such as drug delivery, gene therapy, detection of circulating tumor cells, imaging, cancer immune–therapy, targeted protein degradation.[1] Here, we demonstrated the utilities of compound **5** with two applications: targeted drug delivery and photo-dynamic therapy (PDT). Doxorubicin (Dox) is a widely used chemotherapy drug that intercalates DNA double helices, thereby inhibiting DNA replication, and it has been used in numerous targeted delivery applications.[51] DNA is one of the earliest carriers for targeted delivery of cytotoxic compounds, including Dox.[52] Besides DNA, other types of nucleic acid carriers have also been used, such as aptamers, plasmids, DNA nanostructures, and siRNAs.[51]

Dox intercalates into DNA double helices with high affinity. After internalization, Dox-loaded DNA carrier will be trafficked through endosome to lysosome, and the unloading of Dox is through a combination of mechanisms:[51,53] The low-pH microenvironment of the late endosome and lysosome triggers a change of DNA structure or denature the DNA duplex to release the Dox; the DNA complex can be gradually degraded by intracellular nucleases; and passive dissociation of Dox from the DNA may be a contributing mechanism because of the negligible concentrations of Dox inside the cells.[53] First, we verified that MDA-MB-231 and MCF-7 cells are both sensitive to Dox with similar IC_{50}'s (Figure S34). Next, a 16-nt DNA carrying compound **5** (**DNA-5-Dox**), a photo-reactive CP DNA (31-nt), and a C/G-rich vehicle hairpin DNA (21-bp at the duplex region) were hybridized to form the delivery probe (Figure 6e). A probe without the small molecule was used as the negative control. The probe was incubated with Dox and a 1:10 (probe : Dox) loading ratio appeared to be optimal based on fluorescence quenching (Figure S35). The Dox-loaded probes were incubated with the cells (5 μM, 4 °C, 1.5 hrs.), briefly UV-irradiated, and then washed with cold PBS buffer and then cultured in drug-free fresh medium at 37 °C for 24 h before the cell viability was determined using the CCK-8 assay.[54] As shown in Figure 6f, the probe with compound **5** exhibited selective killing of MDA-MB-231 cells over MCF-7 cells, but not the control probe. Dox and other payload molecules can be directly conjugated with cell-targeting ligands for targeted delivery without a DNA carrier.[53] However, the conjugate design needs to consider several implications, such as chemical modification of the ligand and the payload molecule and the impact of the linker and/or the spacer on cell-binding affinity and specificity.[55] It may take multiple rounds of conjugate synthesis, testing, and optimization. Here, Dox non-covalently intercalates in the DNA, which avoids chemical modification and can release unmodified Dox in the cell. As a test, we synthesized an "off-DNA" conjugate of compound **5** with Dox (**5-Dox**; Figure S36) and the conjugate exhibited relatively higher cytotoxicity towards MDA-MB-231 than MCF7 cells, suggesting that it is possible to directly conjugate compound **5** with a payload molecule for targeted delivery. PDT has been used in cancer treatment for many years.[56] PDT agents typically comprise a photosensitizer (PS) and a targeting moiety connected through a linker. The targeting moiety binds to the cell, and then light irradiation (600–800 nm) generates cytotoxic reactive oxygen species (ROS) to trigger cell death.[57] The ROS generation can either be inside the cell after PS internalization or in proximity to the cell surface.[58] As shown in Figure 6g, a 16-nt DNA carrying compound **5** (**DNA-5-PDT**), a photo-reactive CP DNA (31-nt), and a DNA with a photo-sensitizer methylene blue (MB) hybridized to form the PDT probe. MB is a widely used PS that can generate cytotoxic single oxygen species ($^1O_2$; quantum yield: ~0.52).[57] Under PDT condition, the probe with compound **5** sensitized MDA-MB-231 cells and induced more significant cell death than MCF-7 cells (Figure 6h). Collectively, these experiments demonstrated that the hit compounds have the potential to be used as cell-targeting ligands. However, it is important to note that the trityl group in compound **5** may incur non-selective interactions and metabolic instability, e.g., sensitivity to the acidic microenvironment of cancer cells, which will limit its therapeutic applications. Further structural modifications are necessary to mitigate these issues.

Conclusion

We have shown that DELs can be selected against the cell surface without predefined targets. This approach resembles target-agnostic screening using biological display and OBOC libraries with live cells.[5] DELs generally contain more diverse chemotypes than biological display libraries. Moreover, most DELs are in the solution phase and have larger library sizes than OBOC libraries. It should be noted that OBOC-DELs have recently been developed and they also have relatively smaller library sizes. Unbiased DEL selections on the cell surface are expected to discover novel cell-selective small molecule ligands. Our results showed that the selections gave distinctly different enrichment profiles on cancer cells of different invasive properties. A

comparative analysis identified cell-specific compounds that can be used for targeted cell delivery without the knowledge of their cellular receptors. Furthermore, we performed target identification of one of the ligands (compound **5**) and identified α-enolase as the cell-surface receptor. While α-enolase is already known to be implicated in cancer cell migration and invasion, this study has demonstrated that DELs have potential to be utilized as a tool to explore biology beyond ligand/inhibitor discovery. Typically, after a DEL selection, the hit compounds will be resynthesized off-DNA for hit validation and biological testing. Here, we show that the DNA tag can be leveraged for assembling the delivery vehicle as well as target identification. However, the DNA tag is not necessary and could be removed, since the DNA conjugation site can be conveniently used to attach labels or payloads, such as radionuclides, to develop anti-cancer theranostic agents.

Several points need to be noted. First, unlike regular DEL selections, the abundance of cell-surface proteins and other biomolecules is a confounding factor. The ligands with moderate binding affinities to the targets with high abundance may be more enriched than ligands with higher affinities binding to the targets with very low abundance. Hence, the enrichment fold is a combination of both binding affinity and the effective target concentration on the cell.[12g] This may not be a major concern if the objective is to identify cell-specific small molecules, rather than the ligands specific for individual protein targets. Second, the identified ligands may bind to non-protein biomolecules on the cell-surface. Proteinase K or trypsin may be used to elute protein binders, and the enrichment profile can be compared with the one using the "general elution" conditions (heating or sonication).[50] In this study, we observed that compound **6**'s binding to MDA-MB-231 cells was not significantly reduced by trypsin treatment of the cell surface. However, identifying non-protein receptors will be challenging because it often requires prior knowledge of the putative targets.[50] Third, cell-based selections have lower reproducibility due to the target's heterogeneity, as observed in this study and also in previous reports.[12d,e,i,16] Here, we selected the compounds reproducibly enriched in at least two replicates and then ranked the compounds based on *z*-score comparison. More sophisticated data analysis methods, such as machine learning,[50] is expected to facilitate hit identification from cell-based selection and may even generate unique enrichment "fingerprints" for specific cell types or properties. Fourth, the trityl group in compound **5** may lead to non-selective binding and metabolic instability, limiting its use as a cell-targeting ligand in targeted delivery applications. Therefore, it is important to examine the compound structure and prioritize hit selection and characterization to avoid or minimize these potential issues. Currently, we are applying the selection method to a larger panel of cell lines of different types, properties, and cell states with a larger collection of DELs. We expect that the selections will identify selective ligands without liable structural moieties. We will also implement this approach to identify new cancer biomarkers.

Supporting Information

Additional Supporting Information can be found in a separate document.

Acknowledgements

This work was supported by grants from the GuangDong Basic and Applied Basic Research Foundation General Program (2023A1515010711), Research Grants Council of Hong Kong SAR, China (AoE/P-705/16, 17301118, 17111319, 17303220, 17300321, 17300423, C7005-20G, C7016-22G, C7035-23G, N_HKU702/23, and T12-705-24-R), the Shenzhen Bay 37Laboratory, Shenzhen, China (SZBL2020090501008), NSFC of China (91953203, 22377139), and Shanghai Municipal Science and Technology Major Project. We acknowledge the support from "Laboratory for Synthetic Chemistry and Chemical Biology" under the Health@InnoHK Program and State Key Laboratory of Synthetic Chemistry by Innovation and Technology Commission, Hong Kong SAR, China.

Conflict of Interest

The authors declare no conflict of interest.

Data Availability Statement

Data are available in article supplement materials. Raw sequencing data and source files are also available in a public depository (Figshare; DOI:10.25442/hku.28022942)

Keywords: DNA-encoded chemical libraries · drug discovery · high-throughput screening · targeted drug delivery · target identification

[1] M. T. Manzari, Y. Shamay, H. Kiguchi, N. Rosen, M. Scaltriti, D. A. Heller, *Nat. Rev. Mater.* **2021**, *6*, 351–370.
[2] B. P. Gray, K. C. Brown, *Chem. Rev.* **2014**, *114*, 1020–1081.
[3] a) Z. Fu, S. Li, S. Han, C. Shi, Y. Zhang, *Signal Transduct. Tar. Therapy* **2022**, *7*, 93; b) R.-M. Lu, Y.-C. Hwang, I. J. Liu, C.-C. Lee, H.-Z. Tsai, H.-J. Li, H.-C. Wu, *J. Biomed. Sci.* **2020**, *27*, 1.
[4] a) M. A. Tabrizi, C. M. Tseng, L. K. Roskos, *Drug Discovery Today* **2006**, *11*, 81–88; b) R. Jefferis, *J. Immunol. Res.* **2016**, *2016*, 5358272.
[5] a) R. Liu, X. Li, W. Xiao, K. S. Lam, *Adv. Drug Delivery Rev.* **2017**, *110–111*, 13–37; b) H. S. Pung, G. J. Tye, C. H. Leow, W. K. Ng, N. S. Lai, *Mol. Biol. Rep.* **2023**, *50*, 4653–4664; c) V. V. Komnatnyy, T. E. Nielsen, K. Qvortrup, *Chem. Commun.* **2018**, *54*, 6759–6771; d) W. Arap, M. G. Kolonin, M. Trepel, J. Lahdenranta, M. Cardó-Vila, R. J. Giordano, P. J. Mintz, P. U. Ardelt, V. J. Yao, C. I. Vidal, L. Chen, A. Flamm, H. Valtanen, L. M. Weavind, M. E. Hicks, R. E. Pollock, G. H. Botz, C. D. Bucana, E. Koivunen, D. Cahill, P. Troncoso, K. A. Baggerly, R. D. Pentz, K. A. Do, C. J. Logothetis, R. Pasqualini, *Nat. Med.* **2002**, *8*, 121–127; e) D. N. Krag, G. S. Shukla, G. P. Shen, S. Pero, T. Ashikaga, S. Fuller, D. L.

Weaver, S. Burdette-Radoux, C. Thomas, *Cancer Res.* **2006**, *66*, 7724–7733.
[6] a) W. H. Tan, M. J. Donovan, J. H. Jiang, *Chem. Rev.* **2013**, *113*, 2842–2862; b) T. Bing, N. Zhang, D. Shangguan, *Adv. Biosyst.* **2019**, *3*, e1900193; c) Q. Hu, Z. Tong, A. Yalikong, L.-P. Ge, Q. Shi, X. Du, P. Wang, X.-Y. Liu, W. Zhan, X. Gao, D. Sun, T. Fu, D. Ye, C. Fan, J. Liu, Y.-S. Zhong, Y.-Z. Jiang, H. Gu, *Nat. Chem.* **2023**, *16*, 122–131.
[7] L. Wu, Y. Wang, X. Xu, Y. Liu, B. Lin, M. Zhang, J. Zhang, S. Wan, C. Yang, W. Tan, *Chem. Rev.* **2021**, *121*, 12035–12105.
[8] S. Brenner, R. A. Lerner, *Proc. Nat. Acad. Sci. USA* **1992**, *89*, 5381–5383.
[9] J. Nielsen, S. Brenner, K. D. Janda, *J. Am. Chem. Soc.* **1993**, *115*, 9812–9813.
[10] a) L. H. Yuen, R. M. Franzini, *ChemBioChem* **2017**, *18*, 829–836; b) R. A. Goodnow, Jr., C. E. Dumelin, A. D. Keefe, *Nat. Rev. Drug Discovery* **2017**, *16*, 131–147; c) D. Neri, R. A. Lerner, *Annu. Rev. Biochem.* **2018**, *87*, 479–502; d) F. V. Reddavide, M. Thompson, L. Mannocci, Y. X. Zhang, *Aldrichim Acta* **2019**, *52*, 63–74; e) T. Kodadek, N. G. Paciaroni, M. Balzarini, P. Dickson, *Chem. Commun.* **2019**, *55*, 13330–13341; f) J. Ottl, L. Leder, J. V. Schaefer, C. E. Dumelin, *Molecules* **2019**, *24*, 1629; g) M. Song, G. T. Hwang, *J. Med. Chem.* **2020**, *63*, 6578–6599; h) D. T. Flood, C. Kingston, J. C. Vantourout, P. E. Dawson, P. S. Baran, *Isr. J. Chem.* **2020**, *60*, 268–280; i) D. Conole, H. H. J, J. W. M, *Future Med. Chem.* **2021**, *13*, 173–191; j) A. L. Satz, L. Kuai, X. Peng, *Bioorg. Med. Chem. Lett.* **2021**, *39*, 127851; k) V. B. K. Kunig, M. Potowski, M. Klika Skopic, A. Brunschweiger, *ChemMedChem* **2021**, *16*, 1048–1062 ; l) P. R. Fitzgerald, B. M. Paegel, *Chem. Rev.* **2021**, *121*, 7155–7177; m) A. L. Satz, A. Brunschweiger, M. E. Flanagan, A. Gloger, N. J. V. Hansen, L. Kuai, V. B. K. Kunig, X. Lu, D. Madsen, L. A. Marcaurelle, C. Mulrooney, G. O'Donovan, S. Sakata, J. Scheuermann, *Nat. Rev. Methods Primers* **2022**, *2*, 3; n) Y. R. Huang, Y. Z. Li, X. Y. Li, *Nat. Chem.* **2022**, *14*, 129–140; o) M. Dockerill, N. Winssinger, *Angew. Chem. Int. Ed.*, *62*, e202215542; p) Y. K. Sunkari, V. K. Siripuram, T. L. Nguyen, M. Flajolet, *Trends Pharmacol. Sci.* **2022**, *43*, 4–15; q) A. Dixit, H. Barhoosh, B. M. Paegel, *Acc. Chem. Res.* **2023**, *56*, 489–499; r) B. Matsuo, A. Granados, G. Levitre, G. A. Molander, *Acc. Chem. Res.* **2023**, *56*, 385–401; s) A. A. Peterson, D. R. Liu, *Nat. Rev. Drug Discovery* **2023**, *22*, 699–722; t) A. Lessing, D. Petrov, J. Scheuermann, *Trends Pharmacol. Sci.* **2023**, *44*, 817–831; u) X. Yang, J. L. Childs-Disney, M. Paegel, M. D. Disney, *Isr. J. Chem.* **2023**, *63*, e202300073; v) R. Sahu, S. Yadav, S. Nath, J. Banerjee, A. R. Kapdi, *Chem. Commun.* **2023**, *59*, 6128–6147; w) P. Dickson, *ACS Chem. Biol.* **2024**, *19*, 802–808; x) G. W. Collie, M. A. Clark, A. D. Keefe, A. Madin, J. A. Read, E. L. Rivers, Y. Zhang, *J. Med. Chem.* **2024**, *67*, 864–884; y) G. Zhao, M. Zhu, Y. Li, G. Zhang, Y. Li, *Expert Opin. Drug Discovery* **2024**, *19*, 725–740.
[11] a) K. Götte, S. Chines, A. Brunschweiger, *Tetrahedron Lett.* **2020**, *61*, 151889; b) S. Patel, S. O. Badir, G. A. Molander, *Trends Chem.* **2021**, *3*, 161–175; c) D. K. Kolmel, H. Zhu, M. E. Flanagan, S. K. Sakata, A. R. Harris, J. Wan, B. A. Morgan, *Chem. Rec.* **2021**; d) R. J. Fair, R. T. Walsh, C. D. Hupp, *Bioorg. Med. Chem. Lett.* **2021**, *51*, 128339; e) E. Lenci, L. Baldini, A. Trabocchi, *Bioorg. Med. Chem.* **2021**, *41*, 116218; f) R. Adamik, B. Buchholcz, F. Darvas, G. Sipos, Z. Novák, *Chemistry* **2022**, *28*, e202103967.
[12] a) Z. Wu, T. L. Graybill, X. Zeng, M. Platchek, J. Zhang, V. Q. Bodmer, D. D. Wisnoski, J. Deng, F. T. Coppo, G. Yao, A. Tamburino, G. Scavello, G. J. Franklin, S. Mataruse, K. L. Bedard, Y. Ding, J. Chai, J. Summerfield, P. A. Centrella, J. A. Messer, A. J. Pope, D. I. Israel, *ACS Comb. Sci.* **2015**, *17*, 722–731; b) B. Cai, D. Kim, S. Akhand, Y. Sun, R. J. Cassell, A. Alpsoy, E. C. Dykhuizen, R. M. Van Rijn, M. K. Wendt, C. J. Krusemark, *J. Am. Chem. Soc.* **2019**, *141*, 17057–17061; c) B. Cai, A. B. Mhetre, C. J. Krusemark, *Chem. Sci.* **2023**, *14*, 245–250; d) B. Cai, A. El Daibani, Y. Bai, T. Che, C. J. Krusemark, *JACS Au* **2023**, *3*, 1076–1088; e) S. Oehler, M. Catalano, I. Scapozza, M. Bigatti, G. Bassi, N. Favalli, M. R. Mortensen, F. Samain, J. Scheuermann, D. Neri, *Chem. Eur. J.* **2021**, *27*, 8985–8993; f) L. K. Petersen, A. B. Christensen, J. Andersen, C. G. Folkesson, O. Kristensen, C. Andersen, A. Alzu, F. A. Slok, P. Blakskjaer, D. Madsen, C. Azevedo, I. Micco, N. J. V. Hansen, *J. Am. Chem. Soc.* **2021**, *143*, 2751–2756; g) Y. Huang, L. Meng, Q. Nie, Y. Zhou, L. Chen, S. Yang, Y. M. E. Fung, X. Li, C. Huang, Y. Cao, Y. Li, X. Li, *Nat. Chem.* **2021**, *13*, 77–88; h) Y. Gui, C. S. Wong, G. Zhao, C. Xie, R. Hou, Y. Li, G. Li, X. Li, *ACS Omega* **2022**, *7*, 11491–11500; i) Y. Huang, R. Hou, F. S. Lam, Y. Jia, Y. Zhou, X. He, G. Li, F. Xiong, Y. Cao, D. Wang, X. Li, *J. Am. Chem. Soc.* **2024**, *146*, 24638–24653.
[13] a) N. Svensen, J. J. Diaz-Mochon, M. Bradley, *Chem. Biol.* **2011**, *18*, 1284–1289; b) N. Svensen, J. J. Diaz-Mochon, M. Bradley, *Chem. Commun.* **2011**, *47*, 7638–7640.
[14] K. E. Denton, C. J. Krusemark, *MedChemComm* **2016**, *7*, 2020–2027.
[15] K. R. Mendes, M. L. Malone, J. M. Ndungu, I. Suponitsky-Kroyter, V. J. Cavett, P. J. McEnaney, A. B. MacConnell, T. M. Doran, K. Ronacher, K. Stanley, O. Utset, G. Walzl, B. M. Paegel, T. Kodadek, *ACS Chem. Biol.* **2017**, *12*, 234–243.
[16] J. Deng, S. Belyanskaya, N. Prabhu, C. Arico-Muendel, H. Deng, C. B. Phelps, D. I. Israel, H. Yang, J. Boyer, G. J. Franklin, J. L. Yap, K. E. Lind, C. H. Tsai, C. Donahue, J. D. Summerfield, *SLAS Discov* **2024**, *29*, 100171.
[17] M. A. Barry, W. J. Dower, S. A. Johnston, *Nat. Med.* **1996**, *2*, 299–305.
[18] a) H. B. Lowman, *Annu. Rev. Biophys. Biomol. Struct.* **1997**, *26*, 401–424; b) T. Kodadek, N. G. Paciaroni, M. Balzarini, P. Dickson, *Chem. Commun.* **2019**, *55*, 13330–13341.
[19] P. Zhao, Z. Chen, Y. Li, D. Sun, Y. Gao, Y. Huang, X. Li, *Angew. Chem. Int. Ed.* **2014**, *53*, 10056–10059.
[20] a) D. K. Nomura, J. Z. Long, S. Niessen, H. S. Hoover, S. W. Ng, B. F. Cravatt, *Cell* **2010**, *140*, 49–61; b) N. Jessani, Y. Liu, M. Humphrey, B. F. Cravatt, *Proc. Nat. Acad. Sci. USA* **2002**, *99*, 10335–10340; c) O. H. Aina, R. Liu, J. L. Sutcliffe, J. Marik, C. X. Pan, K. S. Lam, *Mol. Pharm.* **2007**, *4*, 631–651; d) M. C. DeRosa, A. Lin, P. Mallikaratchy, E. M. McConnell, M. McKeague, R. Patel, S. Shigdar, *Nat. Rev. Methods Primers* **2023**, *3*; e) S. Xie, W. Sun, T. Fu, X. Liu, P. Chen, L. Qiu, F. Qu, W. Tan, *J. Am. Chem. Soc.* **2023**, *145*, 7677–7691.
[21] Y. Zhou, C. Li, J. Peng, L. Xie, L. Meng, Q. Li, J. Zhang, X. D. Li, X. Li, X. Huang, X. Li, *J. Am. Chem. Soc.* **2018**, *140*, 15859–15867.
[22] J. C. Faver, K. Riehle, D. R. Lancia, Jr., J. B. J. Milbank, C. S. Kollmann, N. Simmons, Z. Yu, M. M. Matzuk, *ACS Comb. Sci.* **2019**, *21*, 75–82.
[23] a) Y. Huang, L. Meng, Q. Nie, Y. Zhou, L. Chen, S. Yang, Y. M. E. Fung, X. Li, C. Huang, Y. Cao, Y. Li, X. Li, *Nat. Chem.* **2021**, *13*, 77–88; b) H. Ma, J. B. Murray, H. Luo, X. Cheng, Q. Chen, C. Song, C. Duan, P. Tan, L. Zhang, J. Liu, B. A. Morgan, J. Li, J. Wan, L. M. Baker, W. Finnie, L. Guetzoyan, R. Harris, N. Hendrickson, N. Matassova, H. Simmonite, J. Smith, R. E. Hubbard, G. Liu, *RSC Med. Chem.* **2022**, *13*, 1341–1349; c) B. Shi, Y. Deng, P. Zhao, X. Li, *Bioconjugate Chem.* **2017**, *28*, 2293–2301.
[24] D. Vullo, A. Innocenti, I. Nishimori, J. r. Pastorek, A. Scozzafava, S. Pastoreková, C. T. Supuran, *Bioorg. Med. Chem. Lett.* **2005**, *15*, 963–969.
[25] Y. Huang, Y. Deng, J. Zhang, L. Meng, X. Li, *Chem. Commun. (Camb.)* **2021**, *57*, 3769–3772.
[26] S. Oehler, *Chem. Eur. J.* **2021**, 8985–8993.

[27] M. A. Clark, R. A. Acharya, C. C. Arico-Muendel, S. L. Belyanskaya, D. R. Benjamin, N. R. Carlson, P. A. Centrella, C. H. Chiu, S. P. Creaser, J. W. Cuozzo, C. P. Davie, Y. Ding, G. J. Franklin, K. D. Franzen, M. L. Gefter, S. P. Hale, N. J. Hansen, D. I. Israel, J. Jiang, M. J. Kavarana, M. S. Kelley, C. S. Kollmann, F. Li, K. Lind, S. Mataruse, P. F. Medeiros, J. A. Messer, P. Myers, H. O'Keefe, M. C. Oliff, C. E. Rise, A. L. Satz, S. R. Skinner, J. L. Svendsen, L. Tang, K. van Vloten, R. W. Wagner, G. Yao, B. Zhao, B. A. Morgan, *Nat. Chem. Biol.* **2009**, *5*, 647–654.
[28] Y. Deng, J. Peng, F. Xiong, Y. Song, Y. Zhou, J. Zhang, F. S. Lam, C. Xie, W. Shen, Y. Huang, L. Meng, X. Li, *Angew. Chem. Int. Ed. Engl.* **2020**, *59*, 14965–14972.
[29] S. Dawadi, N. Simmons, G. Miklossy, K. M. Bohren, J. C. Faver, M. N. Ucisik, P. Nyshadham, Z. Yu, M. M. Matzuk, *Proc. Nat. Acad. Sci. USA* **2020**, *117*, 16782–16789.
[30] K. J. Chavez, S. V. Garimella, S. Lipkowitz, *Breast Dis.* **2010**, *32*, 35–48.
[31] A. V. Lee, S. Oesterreich, N. E. Davidson, *J. Natl. Cancer Inst.* **2015**, *107*.
[32] W. Decurtins, M. Wichert, R. M. Franzini, F. Buller, M. A. Stravs, Y. Zhang, D. Neri, J. Scheuermann, *Nat. Protoc.* **2016**, *11*, 764–780.
[33] J. C. Faver, K. Riehle, D. R. Lancia, Jr., J. B. J. Milbank, C. S. Kollmann, N. Simmons, Z. Yu, M. M. Matzuk, *ACS Comb. Sci.* **2019**, *21*, 75–82.
[34] a) T. I. R. A. Durie, A. H. Kingsbury, *Nature* **1949**, *164*, 786; b) D. Murdock, M. B. Crow, G. A. Ritchie, M. N. Ashfold, *J. Chem. Phys.* **2012**, *136*, 124313.
[35] a) D. Shangguan, Y. Li, Z. Tang, Z. C. Cao, H. W. Chen, P. Mallikaratchy, K. Sefah, C. J. Yang, W. Tan, *Proc. Nat. Acad. Sci. USA* **2006**, *103*, 11838–11843; b) X. Wu, H. Liu, D. Han, B. Peng, H. Zhang, L. Zhang, J. Li, J. Liu, C. Cui, S. Fang, M. Li, M. Ye, W. Tan, *J. Am. Chem. Soc.* **2019**, *141*, 10760–10769.
[36] G. Li, Y. Liu, L. Chen, S. Wu, X. Li, *Angew. Chem. Int. Ed.* **2013**, *52*, 9544–9549.
[37] a) D. Y. Wang, Y. Cao, L. Y. Zheng, L. D. Chen, X. F. Chen, Z. Y. Hong, Z. Y. Zhu, X. Li, Y. F. Chai, *Chem. Eur. J.* **2017**, *23*, 10906–10914; b) J. Zhang, J. Peng, Y. Huang, L. Meng, Q. Li, F. Xiong, X. Li, *Angew. Chem. Int. Ed.* **2020**, *59*, 17525.
[38] S. E. Ong, B. Blagoev, I. Kratchmarova, D. B. Kristensen, H. Steen, A. Pandey, M. Mann, *Mol. Cell. Proteomics* **2002**, *1*, 376–386.
[39] a) L. Prati, M. Bigatti, E. J. Donckele, D. Neri, F. Samain, *Biochem. Biophys. Res. Commun.* **2020**, *533*, 235–240; b) G. Zimmermann, Y. Li, U. Rieder, M. Mattarella, D. Neri, J. Scheuermann, *ChemBioChem* **2017**, *18*, 853–857.
[40] M. Didiasova, D. Zakrzewicz, V. Magdolen, C. Nagaraj, Z. Balint, M. Rohde, K. T. Preissner, M. Wygrecka, *J. Biol. Chem.* **2015**, *290*, 11983–11999.
[41] a) C. K. Huang, Y. Sun, L. Lv, Y. Ping, *Molecular Therapy - Oncolytics* **2022**, *24*, 288–298; b) F. A. Almaguel, T. W. Sanchez, G. L. Ortiz-Hernandez, C. A. Casiano, *Front. Genetics* **2021**, *11*; c) G. Qiao, A. Wu, X. Chen, Y. Tian, X. Lin, *Int. J. Biol. Sci.* **2021**, *17*, 3981–3992.
[42] Q. Ma, H. Jiang, L. Ma, G. Zhao, Q. Xu, D. Guo, N. He, H. Liu, Z. Meng, J. Liu, L. Zhu, Q. Lin, X. Wu, M. Li, S. Luo, J. Fang, Z. Lu, *Proc. Nat. Acad. Sci. USA* **2023**, *120*, e2209435120.
[43] D.-W. Jung, W.-H. Kim, S.-H. Park, J. Lee, J. Kim, D. Su, H.-H. Ha, Y.-T. Chang, D. R. Williams, *ACS Chem. Biol.* **2013**, *8*, 1271–1282.
[44] Y. Cheng, W. H. Prusoff, *Biochem. Pharmacol.* **1973**, *22*, 3099–3108.
[45] a) E. Cayir, A. Erdemir, E. Ozkan, M. Topuzogullari, Z. B. Bolat, A. Akat, D. Turgut-Balik, *Mol. Biotechnol.* **2014**, *56*, 689–696; b) R. B. Brandt, Laux, J. E., & Yates, S. W., *Biochem. Med. Metab. Biol.* **1987**, *37*, 344–349.
[46] N. Sheokand, H. Malhotra, S. Kumar, V. A. Tillu, A. S. Chauhan, C. I. Raje, M. Raje, *J. Cell Sci.* **2014**, *127*, 4279–4291.
[47] A. Bednarek, D. Satala, M. Zawrotniak, A. H. Nobbs, M. Rapala-Kozik, A. Kozik, *Int. J. Mol. Sci.* **2024**, *25*.
[48] a) Y. Du, J. Zhou, J. Fan, Z. Shen, X. Chen, *J. Proteome Res.* **2009**, *8*, 2211–2217; b) P. C. Havugimana, G. T. Hart, T. Nepusz, H. Yang, A. L. Turinsky, Z. Li, P. I. Wang, D. R. Boutz, V. Fong, S. Phanse, M. Babu, S. A. Craig, P. Hu, C. Wan, J. Vlasblom, V. U. Dar, A. Bezginov, G. W. Clark, G. C. Wu, S. J. Wodak, E. R. Tillier, A. Paccanaro, E. M. Marcotte, A. Emili, *Cell* **2012**, *150*, 1068–1081.
[49] D. Shangguan, Y. Li, Z. Tang, Z. C. Cao, H. W. Chen, P. Mallikaratchy, K. Sefah, C. J. Yang, W. Tan, *Proc. Nat. Acad. Sci. USA* **2006**, *103*, 11838–11843.
[50] N. Zhao, M. C. Woodle, A. J. Mixson, *J. Nanomed. Nanotechnol.* **2018**, *9*.
[51] a) A. Trouet, D. Deprez-de Campeneere, C. De Duve, *Nat New Biol* **1972**, *239*, 110–112; b) A. Trouet, D. Deprez-de Campeneere, M. de Smedt-Malengreaux, G. Atassi, *Eur J Cancer (1965)* **1974**, *10*, 405–411.
[52] a) J. Wen, W. Tao, S. Hao, S. P. Iyer, Y. Zu, *Leukemia* **2016**, *30*, 987–991; b) V. Bagalkot, O. C. Farokhzad, R. Langer, S. Jon, *Angew. Chem. Int. Ed. Engl.* **2006**, *45*, 8149–8152; c) P. Sandal, L. Kumari, P. Patel, A. Singh, D. Singh, G. D. Gupta, B. D. Kurmi, *Assay Drug Dev. Technol.* **2023**, *21*, 137–156.
[53] M. H. Ge, X. H. Zhu, Y. M. Shao, C. Wang, P. Huang, Y. Wang, Y. Jiang, Y. Maimaitiyiming, E. Chen, C. Yang, H. Naranmandura, *Biomater. Sci.* **2021**, *9*, 1313–1324.
[54] a) S. S. Yu, K. Athreya, S. V. Liu, A. V. Schally, D. Tsao-Wei, S. Groshen, D. I. Quinn, T. B. Dorff, S. Xiong, J. Engel, J. Pinski, *Clin. Genitourin. Cancer* **2017**, *15*, 742–749; b) G. Emons, G. Gorchev, P. Harter, P. Wimberger, A. Stähle, L. Hanker, F. Hilpert, M. W. Beckmann, P. Dall, C. Gründker, H. Sindermann, J. Sehouli, *Int J Gynecol Cancer* **2014**, *24*, 260–265; c) C. Zhuang, X. Guan, H. Ma, H. Cong, W. Zhang, Z. Miao, *Eur. J. Med. Chem.* **2019**, *163*, 883–895; d) J. Zhang, F. Hu, O. Aras, Y. Chai, F. An, *ChemMedChem* **2024**, *19*, e202300720; e) T. Wang, M. Li, R. Wei, X. Wang, Z. Lin, J. Chen, X. Wu, *Mol. Pharm.* **2024**, *21*, 1038–1055; f) M. Srinivasarao, C. V. Galliford, P. S. Low, *Nat. Rev. Drug Discovery* **2015**, *14*, 203–219.
[55] D. E. J. G. J. Dolmans, D. Fukumura, R. K. Jain, *Nat. Rev. Cancer* **2003**, *3*, 380–387.
[56] T. C. Pham, V.-N. Nguyen, Y. Choi, S. Lee, J. Yoon, *Chem. Rev.* **2021**, *121*, 13454–13619.
[57] a) W. Ma, S.-N. Sha, P.-L. Chen, M. Yu, J.-J. Chen, C.-B. Huang, B. Yu, Y. Liu, L.-H. Liu, Z.-Q. Yu, *Adv. Healthcare Mater.* **2020**, *9*, 1901100; b) W. Zhang, Y. Huang, Y. Chen, E. Zhao, Y. Hong, S. Chen, J. W. Y. Lam, Y. Chen, J. Hou, B. Z. Tang, *ACS Appl. Mater. Interfaces* **2019**, *11*, 10567–10577; c) Y. Bu, T. Xu, X. Zhu, J. Zhang, L. Wang, Z. Yu, J. Yu, A. Wang, Y. Tian, H. Zhou, Y. Xie, *Chem. Sci.* **2020**, *11*, 10279–10286.
[58] a) N. Thapa, S. Kim, I. S. So, B. H. Lee, I. C. Kwon, K. Choi, I. S. Kim, *J. Cell. Mol. Med.* **2008**, *12*, 1649–1660; b) E. N. Peletskaya, V. V. Glinsky, G. V. Glinsky, S. L. Deutscher, T. P. Quinn, *J. Mol. Biol.* **1997**, *270*, 374–384; c) C. Laumonier, J. Segers, S. Laurent, A. Michel, F. Coppee, A. Belayew, L. V. Elst, R. N. Muller, *J Biomol Screen* **2006**, *11*, 537–545; d) R. Shao, C. Xiong, X. Wen, J. G. Gelovani, C. Li, *Mol. Imaging* **2007**, *6*, 417–426.

Manuscript received: October 31, 2024
Accepted manuscript online: January 10, 2025
Version of record online: January 17, 2025